Pole-Placement Self-Tuning Control of a Fixed-Bed Autothermal Reactor

Part II: Multivariable Control

The multiinput/multioutput pole-placement self-tuning controller (MIMO PPSTC) previously developed by McDermott and Mellichamp is used to control a fixed-bed autothermal reactor with internal countercurrent heat exchange. The performance of the controller is demonstrated using step changes in the set points and in the primary disturbance variables. It is shown that the complete temperature profile can be maintained by controlling two temperatures in the catalyst bed: one just before the hot spot and the other at the exit of the bed. Simulated results using a 36th-order nonlinear reactor model operating at both an open-loop upper stable steady state and an open-loop unstable steady state are presented. Experimental results for a fixed-bed autothermal reactor operating at an upper stable state are presented.

P. E. McDermott, D. A. Mellichamp, R. G. Rinker
Department of Chemical and Nuclear Engineering
University of California
Santa Barbara, CA 93106

SCOPE

Control of catalytic fixed-bed reactors is a difficult and challenging problem. These systems are typically distributed in nature and possess extreme nonlinearities. Due to complex interactions between thermal and kinetic processes, fixed-bed reactors exhibit so-called wrong way (or inverse) response characteristics, which further compounds the control problem.

In recent years, several multivariable control approaches have been successfully demonstrated experimentally. Sørensen (1977), Clement et al. (1980), and Sørensen et al. (1980) have considered the optimal control of a nonadiabatic fixed-bed reactor. Silva et al. (1979) investigated the linear quadratic Gaussian control of a two-bed catalytic reactor. A multivariable proportional-integral control scheme was investigated by Wallman et al. (1979) on the same two-bed reactor. Jutan et al. (1977a, b, c, d) considered the control of a nonadiabatic butane hydrogenolysis reactor by means of a multivariable linear quadratic feedback controller. Wong et al. (1983) studied the control of a fixed-bed autothermal reactor operating at an open-loop unstable steady state using modal control theory.

In most multivariable control techniques, a mathematical model of the system is required in order to design the controller. The usual approach for reactor control is to start with a phenomenological model of the system, discretize the spatial derivatives, and then use model reduction to obtain a low-order model suitable for controller design. Before the model reduction step can be done, off-line parameter estimation must be performed to determine any unknown model parameters. This method of obtaining a model is often very time-consuming and costly. Furthermore, the resulting model is only valid in the vicinity of the operating point at which it was developed. If reactor operating conditions change, the model and the controller are no longer applicable.

Recently, major developments have been made in the area of multivariable self-tuning control. These controllers are attractive because they are easy to implement (no *a priori* process model is required), and they are applicable over a wide range of operating conditions.

Correspondence concerning this paper should be addressed to R. G. Rinker.

A few applications of multivariable self-tuning controllers have been made to chemical processes. Several investigators (Dahlqvist, 1979, 1981; Morris et al., 1980, 1982; and Gerry et al., 1983) have considered the control of distillation columns. Buchholt and Kümmel (1981) investigated the multivariate self-tuning control of a double-effect evaporator. Koivo et al. (1981) considered the self-tuning control of a concentration-flow process.

Among the applications of self-tuning controllers to fixed-bed chemical reactors, most have used single-input/single-output algorithms (Åström, 1978; Harris et al., 1980; Lee and Lee, 1985) except for the application of a multivariable self-tuning controller due to Hallager and Jørgensen (1981). They considered a linear, quadratic optimal controller based on a model identified on-line using recursive least squares.

In this paper, the control of a fixed-bed autothermal reactor conducting the water-gas shift reaction is considered. Controlled operation of the reactor at an upper stable steady state and at an unstable steady state is demonstrated using the multivariable pole-placement self-tuning controller developed by McDermott and Mellichamp (1984) on both a 36th-order nonlinear reactor model and an experimental autothermal reactor.

CONCLUSIONS AND SIGNIFICANCE

Multivariable, self-tuning control of a fixed-bed autothermal reactor has been demonstrated. Simulation results using a 36th-order nonlinear model operating at an upper stable steady state have shown that controlling two temperatures in the catalyst bed, one immediately before the hot spot and one at the exit, is sufficient to maintain the complete temperature profile in the reactor during upset periods. Simulation studies have also been used to compare two different control structures: using heat input at the entrance of the catalyst bed to control the temperature just ahead of the hot spot, and using either the feed flow rate or heat input to the feed to control the bed exit temperature. At both the upper stable state and the unstable state, the two control structures worked equally well with the simulated system for step changes in the set points, and for step changes in the load variable at the upper stable state. However, at the unstable state large changes were required in the feed flow rate when it was manipulated, causing the system nonlinearities to become important and greatly reducing the effectiveness of the controller. When the feed heater was manipulated, excellent set point responses were attained.

An experimental autothermal reactor operating at an upper stable state was then used to verify the performance of the controller using feed flow rate as the manipulated variable. The response of the system for step changes in the set points was very similar to the simulations, but a larger control action was observed for the experimental system. Control at an unstable state was not possible due to the excitation of strong nonlinearities and the imposition of important physical constraints. Where operation was found to be feasible, the multivariable pole-placement self-tuning controller demonstrated excellent robustness characteristics, for example in the ability to use quite low-order models (few parameters to identify on-line). The dynamic decoupler has been shown to be effective in minimizing interactions between the loops, even for major changes in the manipulated variables, so long as the nonlinearities of the reactor were not extreme. Finally, the new idea of self-tuning the closed-loop poles online to yield optimal step changes in the set points, and to reduce loop interactions, worked very well.

The Autothermal Reactor

The reactor considered in this paper is a fixed-bed autothermal reactor with internal countercurrent heat exchange, schematically shown in Figure 1. Feed gases enter at the bottom of the reactor, travel up through an annular section, turn around at the top of the reactor, and pass down through the catalyst bed. Heat that is generated in the bed by an exothermic reaction is transferred radially, preheating the feed gases in the annulus. This thermal coupling is responsible for the existence of three steady states; an upper and a lower stable state and an intermediate, unstable state.

Manipulated variables that are available for potential use in multivariable controller configurations are:

1. A small heater at the entrance to the catalyst bed (the top heater)
2. A small heater at the entrance to the reactor (the bottom heater)
3. The total feed flow rate.

The controlled variables are catalyst bed temperatures at 0.707 of the bed radius from the centerline of the bed, and located at two axial positions. The eight measurement locations, at 0.048, 0.115, 0.206, 0.316, 0.437, 0.563, 0.794, and 0.991 from the top of the bed, correspond to collocation points used in the reactor model. More details concerning the experimental system can be found in Part I.

A mathematical model of the reactor has been developed that consists of five partial differential equations in three dimensions

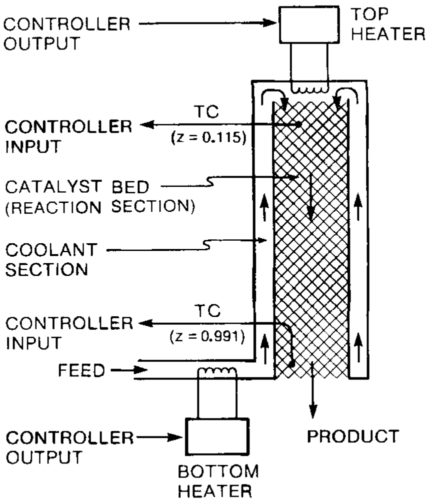

Figure 1. Diagram and controller configuration of autothermal reactor with internal countercurrent heat exchange (ARICHE).

(axial and radial locations plus time) describing material and energy balances in the reactor (Bonvin et al., 1983; McDermott, 1984). Using orthogonal collocation to eliminate the two spatial coordinates, a 36th-order nonlinear ordinary differential equation model was obtained.

Controller Design and Implementation

Controller design

The controller used in this study is the multiinput/multioutput pole-placement self-tuning controller developed by McDermott and Mellichamp (1984). As the complete and more general derivation can be found elsewhere, only a short description is given here.

For the reactor applications, the controller design assumes that the process can be described by a two-input/two-output, linear, discrete-time, randomly disturbed model of the form

$$\underline{A}(z^{-1})Y(t) = [B^{ij}(z^{-1})z^{-k^{ij}_{\min}}]U(t) + X(t) \tag{1}$$

where U and Y are 2-vectors of the deviations from mean system input and output, respectively; $\underline{A}(z^{-1})$ is a 2×2 diagonal matrix polynomial; $\underline{B}(z^{-1})$ is a 2×2 matrix polynomial; and $k_{\min}$ is the minimum expected time delay between the i, j output-input pair. The signal $X(t)$ is a disturbance term that is assumed to have the form

$$X(t) = \underline{C}(z^{-1})\xi(t) + d \tag{2}$$

where $\underline{C}(z^{-1})$ is a 2×2 diagonal matrix polynomial, ξ is a 2-vector of uncorrelated random sequence with zero mean, and d is a 2-vector of constant offsets. Since the controller is based on a multiloop configuration, the outputs and inputs are assumed to be paired: u^1 with y^1 and u^2 with y^2. A dynamic decoupler then attempts to minimize the loop interactions.

The control law is determined so as to minimize a scalar objective function

$$I = \min \epsilon\{[\phi^i(t + k^{ii}_{\min})]^T[\phi^i(t + k^{ii}_{\min})]\} \tag{3}$$

where $[\phi^i(t + k^{ii}_{\min})]$ is a 2-vector of generalized outputs defined as

$$[\phi^i(t + k^{ii}_{\min})] = \underline{P}(z^{-1})[y^i(t + k^{ii}_{\min})] + \underline{Q}(z^{-1})U(t) - \underline{R}(z^{-1})Y_r(t) \tag{4}$$

$\underline{P}(z^{-1})$ and $\underline{R}(z^{-1})$ are arbitrary diagonal matrix polynomials, $\underline{Q}(z^{-1})$ is an arbitrary 2×2 matrix polynomial, and $Y_r(t)$ is a 2-vector of set points.

Equation 4 cannot be substituted directly in the objective function since unknown future data are required. However, an optimal $k^{ii}_{\min}$ step-ahead predictor of $[\phi^i(t + k^{ii}_{\min})]$ can be derived to obtain the control law

$$\underline{S}_D U(t) + [S^{ij}_{UL} z^{(k^{ii}_{\min} - k^{ij}_{\min})}]\, U(t) = -\underline{F}Y(t) + \underline{CR}Y_r(t) - \gamma \tag{5}$$

where

$$\underline{S}_D = \underline{EB}_D + \underline{CQ}_D$$
$$\underline{S}_{UL} = \underline{EB}_{UL} + \underline{CQ}_{UL}$$
$$\gamma = \underline{E}(z^{-1} = 1)d$$

The subscript D refers to the diagonal elements of a matrix polynomial, and UL refers to the upper and lower triangular elements.

The closed-loop behavior of the process can be found by substituting the control law, Eq. 5, into the process model, Eq. 1, to obtain

$$(\underline{B}_D\underline{P} + \underline{Q}_D\underline{A})[y^i(t + k^{ii}_{\min})] = \underline{B}_D\underline{R}Y(t) + \underline{Q}_D d + \underline{B}_D\underline{C}^{-1}(\underline{E}d - \gamma) + [(Q^{ii}_D B^{ij}_{UL} - B^{ii}_D Q^{ij}_{UL})z^{(k^{ii}_{\min} - k^{ij}_{\min})}]\,U(t) + (\underline{B}_D\underline{E} + \underline{CQ}_D)[\xi^i(t + k^{ii}_{\min})] \tag{6}$$

Equation 6 is not, strictly speaking, a closed-loop equation since it contains an input term on the righthand side. However, the dynamic decoupler attempts to set this term to $\underline{O}$.

The concept behind the pole-placement design criterion is to choose $\underline{P}$ and $\underline{Q}$ such that the closed-loop poles of the diagonal system are positioned at prespecified locations

$$\underline{B}_D\underline{P} + \underline{Q}_D\underline{A} = V \tag{7}$$

polynomials. The roots of $V(z)$ are the desired closed-loop poles for the i, i input-output pair.

In order that each input not disturb the outputs of other loops and to retain the validity of the placement of the poles of the diagonal system, the crosscoupling terms must vanish from Eq. 6. Thus, the requirements are

$$Q^{11}B^{12} - B^{11}Q^{12} = 0 \quad \text{and} \quad Q^{22}B^{21} - B^{22}Q^{21} = 0 \tag{8}$$

Equating coefficients of like powers of z^{-1} results in two systems of linear equations for the unknown coefficients of Q^{12} and Q^{21}. As each system is overdetermined (whenever $n_B ii > 0$), linear least-squares must be used.

The straightforward least-squares solution reduces dynamic interactions between loops, but in general does not guarantee static decoupling unless $Q^{ij}_{UL}(1) = 0$ for $i, j = 1, 2$. This constraint is easily included in the least-squares formulation.

The controller, Eq. 5, has integral action as long as a good estimate of the offset level, $\boldsymbol{d}$, is available. For the case when a good estimate of $\boldsymbol{d}$ is not available, such as right after a load disturbance enters the process, or when $\boldsymbol{d}$ is not persistently exciting, i.e., the disturbance does not excite enough of the system dynamics to permit identification of the model, the closed-loop system exhibits steady state offset. An alternative approach that eliminates the possibility of offset is to assume that $X(t)$ is modeled as an integrated moving-average process

$$\Delta X(t) = \underline{C}(z^{-1})\xi(t) \tag{9}$$

where

$$\Delta = (1 - z^{-1})$$

Using Eq. 9 in the derivation of the controller yields the following new control law

$$\underline{\boldsymbol{S}}_D^{\dagger}\boldsymbol{U}(t) + [S_{UL}^{\dagger ij} z^{(k_{\min}^{ii} - k_{\min}^{ij})}]\, \boldsymbol{U}(t) = -\underline{\boldsymbol{F}}^{\dagger}\boldsymbol{Y}(t) + \underline{\boldsymbol{CRY}}_r(t) \tag{10}$$

where

$$\underline{\boldsymbol{S}}_D^{\dagger} = \Delta\underline{\boldsymbol{E}}^{\dagger}\underline{\boldsymbol{B}}_D + \underline{\boldsymbol{CQ}}_D$$
$$\underline{\boldsymbol{S}}_{UL}^{\dagger} = \Delta\underline{\boldsymbol{E}}^{\dagger}\underline{\boldsymbol{B}}_{UL} + \underline{\boldsymbol{CQ}}_{UL}$$

Since $\underline{\boldsymbol{Q}}(1) = 0$ (as specified above), the controller now has a pole at $z = 1$, i.e., contains an intergrator in each loop.

In order to optimize the response of the system to changes in the set points and to reduce loop interactions, the method proposed by McDermott and Mellichamp (1984) in which a single nonzero closed-loop pole is positioned on-line so as to optimize the set point response, can be applied. In this case, a single nonzero closed-loop pole for each loop can be placed so as to minimize an objective function of the form

$$I = \sum_{i=1}^{2}\sum_{j=1}^{N} [y^i(j + k_{\min}^{ii}) - y_r^i(j)]^2 \tag{11}$$

where N represents the time required to obtain the system response to step changes in each of the set points. The remaining poles for each loop are placed at the origin (are made infinitely fast).

In order for the controller to autotune its poles on-line, a measure is needed indicating when to rerun the optimization. Since R^{ii} must be chosen in order to give a unity gain for set point changes, it must change whenever B^{ii} changes (for a given closed-loop pole). Thus, the controller can be instructed to monitor R^{ii} on-line and to reoptimize the poles whenever changes in R^{ii} exceed some prespecified limits.

Control implementation

The parameters of the process model, $\underline{A}(z^{-1})$, $\underline{B}(z^{-1})$, $\underline{C}(z^{-1})$, and $\boldsymbol{d}$ (as required) were identified using recursive extended least-squares with *UD* factorization of the covariance matrix. A pseudorandom binary (PRB) signal was added to the controller output so as to excite the process during the initial stages of the identification. The amplitude of the PRB signal was calculated as a linear function of the trace of the covariance matrix.

During normal operation of the pole-placement controller, control was calculated using Eq. 5. At each time step, a decision was made to determine if $P^{ii}(z^{-1})$ and $Q^{ii}(z^{-1})$ should be recalculated. If the residual of the ith loop, $y^i_{\text{actual}} - y^i_{\text{estimated}}$, was less than σ^i, the standard deviation of the noise of the ith output, then the estimated model was assumed to be a good representation of the process. In this case, the previous values of P^{ii} and Q^{ii} were used. The polynomial identity and the decoupling relations were solved at each time step to account for slight variations in the estimated parameters, in any case.

Whenever the residual exceeded σ^i, a system of simultaneous linear equations, Eq. 7, had to be solved on-line. However, whenever $A^{ii}(z^{-1})$ and $B^{ii}(z^{-1})$ have a common root, the system becomes indeterminant. To ensure that this did not happen during any of the runs, two checks were included in the control program:

1. Whenever the determinant of the system of equations was found to be below a certain threshhold (chosen to be 0.001)
2. Whenever p_0^{ii} (the leading coefficient in the P^{ii} polynomial) changed by more than ± 1, the previous P^{ii} and Q^{ii} polynomial coefficients were again used.

If the residual exceeded the noise level of the ith loop, assumed to be $10\,\sigma^i$, the estimated model no longer could be taken as a good representation of the process. This usually happened after a load disturbance entered the reactor. Covariance resetting, i.e., the addition of a constant diagonal matrix to the covariance matrix, caused a new model to be reidentified. (A factor of 100 $\underline{I}$ was used in all the runs.) However, during this period of reestimation, the parameters varied significantly, and control based on these inaccurate parameters might have caused the closed-loop system to go unstable. Hence, during this period, the most recent previous estimates of the parameters, i.e., those used before the estimation was restarted, were used in the control law given by Eq. 10. Since this controller was based on the old process model, an exponential filter prevented the controller from taking too vigorous control action. The new model was assumed to have converged when the value of the trace had again dropped below 15.

In each of the following runs, the sampling period was chosen to be 60 s for both loops. (The development of the controller does not require that each sampling period be equal.) Table 1 lists the controller and estimator parameters used for the simulation and experimental runs. An eigenvalue analysis of the system (McDermott, 1984) shows that the system is dominantly first-order, so the choice of first-order polynomials for $\underline{A}$ is not unreasonable. This choice also reduces the possibility of a pole-zero cancellation occurring during the identification step. In any case, higher order $\underline{B}$ polynomials can account for more complex behavior. In order to deal with expected changes in the process model, the following techniques were used: covariance resetting, as discussed above, and the fault-detection method of Hägglund (1982). Autotuning of the closed-loop poles was initiated whenever R^{ii} changed by +5 or −10%.

Control at the Upper Stable Steady State

Simulation results—Single-variable control

In the first run, a single-input/single-output pole-placement controller was used in order to compare results with reactor temperature profiles obtained subsequently using multivariable controllers. The measurement location was located at 0.115

Table 1. Controller and Estimator Parameters

	Loop #1	Loop #2	Loop #3
	Controlled Variable		
	$T(z = 0.115)$	$T(z = 0.991)$	$T(z = 0.991)$
	Manipulated Variable		
	Top Heater	Bottom Heater	Feed Flow Rate
Model orders			
n_A^{ii}	1	1	1
n_B^{ii}	3	3	3
n_B^{ij}	3	3	3, 2*
n_C^{ii}	1	1	1
k_{min}^{ii}	1	1, 2*	1
k_{min}^{ij}	1	4, 3*	3, 4**
Max. amplitude of PRBs signal	0.5 W 0.25 W**	10 W 20 W*	$2.50 \times 10^{-6} m^3/s$ $3.33 \times 10^{-6} m^3/s$* $8.34 \times 10^{-6} m^3/s$**
Trace of covariance matrix when PRB signal has its maximum	15	15	15
Absolute value of residual below which P^{ii} and Q^{ii} are constant	0.25 0.15* 0.4**	0.1	0.1 0.05* 0.25**

*Unstable state only
**Experimental run only

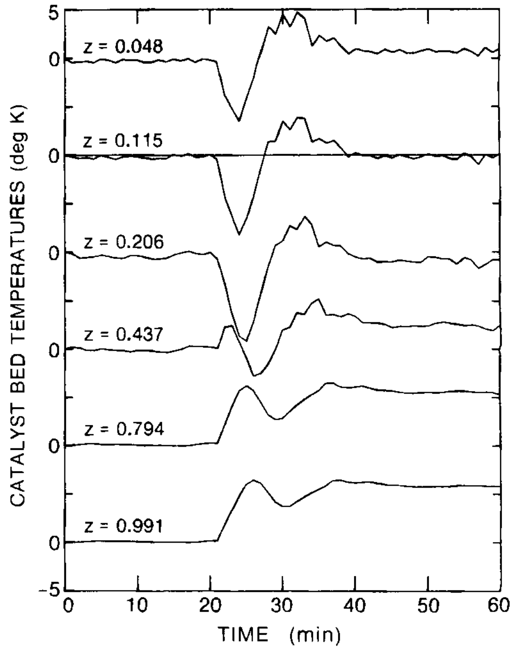

Figure 2. Response of reactor model to a 10% step change in feed flow rate.
Single-input/single-output pole-placement self-tuning controller, upper stable steady state.

dimensionless distance from the top of the catalyst bed and the manipulated variable was selected to be the top heater. The model structure was chosen as follows: $n_A = 1$, $n_B = 3$, $n_C = 1$, $k_{min} = 1$. The sampling period was chosen to be 60 s. Figure 2 shows the results of a 10% step change in the feed flow rate, at $t = 20$ min. The controller is able to handle this rather drastic disturbance very well, and the output has returned to the set point 20 min after the load change entered the process. However, the temperatures in the lower half of the catalyst bed do not return to their original values. Thus, controlling a single temperature in the top half of the bed keeps the reactor from running away or blowing off, but does not guarantee that all temperatures will remain at (or close to) the original values. In order to ensure that the entire temperature profile will remain reasonably constant, a multivariable (MV) controller must be used. We compare these single-variable controller results with those of an analogous MV controller after first discussing MV control structures.

Multivariable control structure development

In order to use the multivariable self-tuning control algorithm outlined above, the structure (i.e., the pairing of inputs and outputs) of the control system must be determined. Using the structural dominance analysis method (Bonvin and Mellichamp, 1982) to analyze the linearized reactor model, it was determined (based on dynamic and static effects [McDermott, 1984]), that the best controller configuration at the upper stable steady state is to control the temperature at $z = 0.206$, $T(z = 0.206)$, using the top heater, and to control the temperature at $z = 0.991$, $T(z = 0.991)$, using the feed temperature. For the unstable state, it was found that the best configuration is to control $T(z = 0.316)$ using the top heater and to control $T(z = 0.991)$ using the feed flow rate.

In the experimental system it is not possible to directly manipulate the feed temperature. Instead, a small heater at the inlet of the reactor is used for control purposes. An empirical first-order transfer function between the heater output and the feed temperature has been found [$G(s) = 2.2/(780\,s + 1)$ deg/W, time in s] and included in the mathematical model to make it more realistic. Hence, the bottom heater was used as the manipulated variable in the following runs, instead of feed temperature. Adding this transfer function has opposing effects on the structural analysis results, i.e., it makes the dynamic results worse but improves the static effects. In any case, since the self-tuning controller works only on input-output data, these differences should not affect the performance of the controller.

The structural analysis showed that the temperature at $z = 0.115$ was found to be only slightly less sensitive than $T(z = 0.206)$ (for the upper stable state) and $T(z = 0.316)$ (for the unstable state). Since the time delay associated with $T(z = 0.115)$ is one-half of that associated with $T(z = 0.206)$, and one-third of that associated with $T(z = 0.316)$, we decided to use $T(z = 0.115)$ in the control structure for operations at both steady states.

Simulation results—Multivariable control

Figure 3 shows the results of the 10% change in the feed flow rate using the multivariable self-tuning controller (the same change made earlier with the single-loop controller). Both loops are very effective in dealing with the load change. However, the control action that is taken by the bottom heater to bring $T(z = 0.991)$ back to its set point causes $T(z = 0.115)$ to require more time to return to its set point. The reason that the

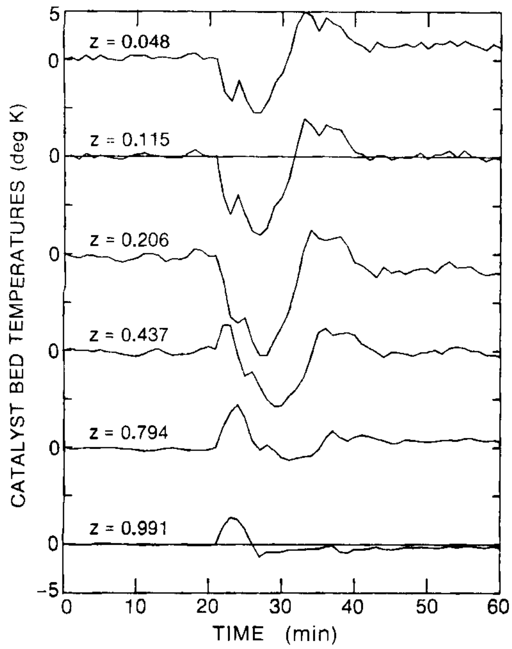

Figure 3. Response of reactor model to a 10% step change in feed flow rate.

Multiinput/multioutput pole-placement self-tuning controller, upper stable steady state.

top heater does not compensate for the change in the bottom heater immediately is that the feed flow rate changes cause covariance resetting to be initiated in the top loop. During this period, the old model was used for control purposes and the controller output was filtered. Thus, the complete input signal required for decoupling was not used.

After all the transients have died out, the temperatures in the catalyst bed are almost identical to their initial values, a considerable improvement over the single-loop controller (compare Figures 2 and 3). Thus, the reason for using the dual-loop controller is validated. A comparison of exit conversions reveals that the single-loop controller yields a slightly better value of conversion than the dual-loop controller (~1% higher). The reason is that the higher exit temperature for the single-loop controller enhances the reaction rate in the lower half of the reactor. However, note that a disturbance that would lower the temperatures in the lower half of the reactor would mean less conversion for the single-loop controller.

We now see that controlling the temperature immediately before the hot spot and at the bed exit does not always lead to improve conversions. Controlling these temperatures essentially specifies the shape of the profile, so this control strategy is well suited for use with an overall supervisory approach, such as the approach of Lee and Lee (1985).

Figure 4 shows the response of the system for set point changes in each of the loops. Since the closed-loop poles have been autotuned to give optimal step changes in the set points, each is followed very closely. The decoupler is effective in dealing with the top heater–$T(z = 0.991)$ interaction very well. However, it is not as effective in the other direction. The interactions are more apparent in $T(z = 0.115)$ because a large amount of control action is required from the bottom heater when the associated set point is changed. Since the model was identified using much lower input levels, it apparently is only partially

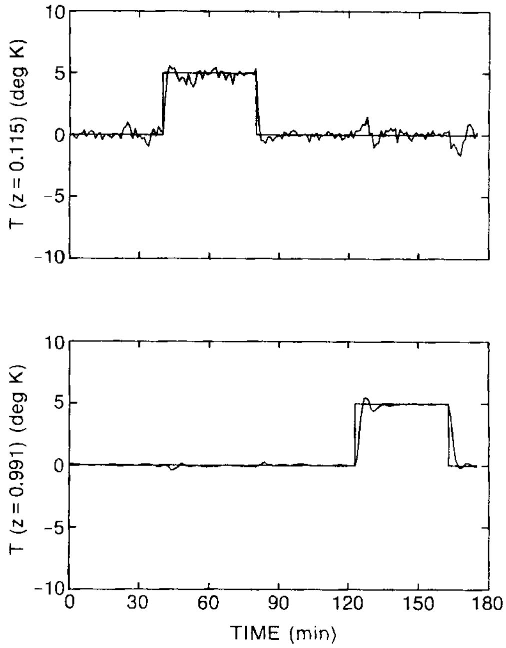

Figure 4. Response of reactor model to a step change in set points.

Bottom heater as second manipulated variable, upper stable steady state.

adequate for such drastic changes. Nonetheless, the interactions are kept to reasonable levels.

In order to study the alternate dual-loop control structure, the feed flow rate replaced the bottom heater as the second manipulated variable. Figure 5 shows the response of the system for set point changes in each loop. In this case, both loops do exception-

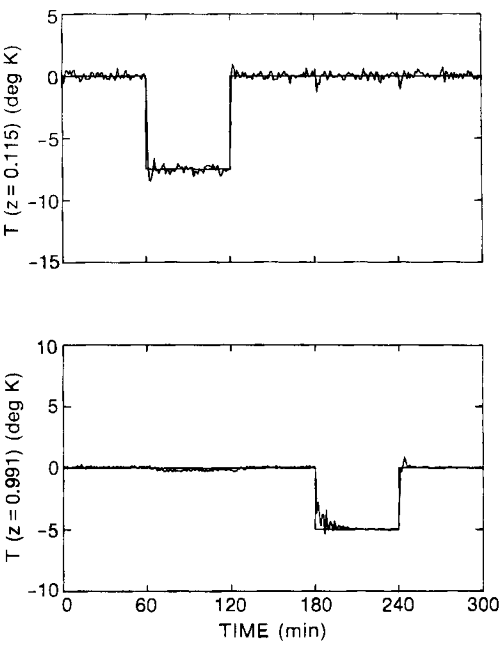

Figure 5. Response of reactor model to a step change in set points.

Feed flow rate as second manipulated variable, upper stable steady state.

ally well, i.e., both set points are followed closely and the interactions are quite small. The slight offset that persists in $T(z = 0.991)$ during the set point change in $T(z = 0.115)$ results from the fact that the nonlinearities excited by the large set point change are not well modeled. One way of dealing with this problem is to use the integral controller, Eq. 10, in the second loop so that the offset does not persist.

Small step changes in the bottom heater produce changes in the catalyst bed temperatures that are very slow-acting, very much like system drift. Hence, this variable is a perfect candidate for showing the effect of a disturbance that is not persistently exciting. Figure 6 shows the response of the system to a load change, an 8 W step change in the bottom heater output at $t = 10$ min, where Eq. 2 is used as the disturbance model. Since the effect of this type of disturbance is very much like a drift in the system, we would expect some difficulties when this disturbance model is used. However, the controller appears to be able to handle the disturbance very well.

Since this type of disturbance most seriously affects the parameter estimates, the behavior of the model parameters must be considered. Figure 7a shows that, for the top loop, the parameters appear to be well-behaved. However, a closer inspection reveals that a_1^{11} has changed from -0.98 to -1.2. Therefore, the open-loop pole has migrated from inside the unit circle, $z = 0.98$, to outside the unit circle, $z = 1.2$, meaning that, in order to model the drift in the system, the estimator had to force the system open-loop model to be unstable. We also notice that d^1, the estimate of the constant offset, has not changed. For the bottom loop, all of the parameter estimates (except d^2) have changed in order to model the apparent drift in the system.

Figure 8 shows that the response of the system to the same load change, when Eq. 9 is used as the disturbance model, is similar to the previous response (compare Figures 6 and 8). However, in this case there is more oscillation in the inputs; hence,

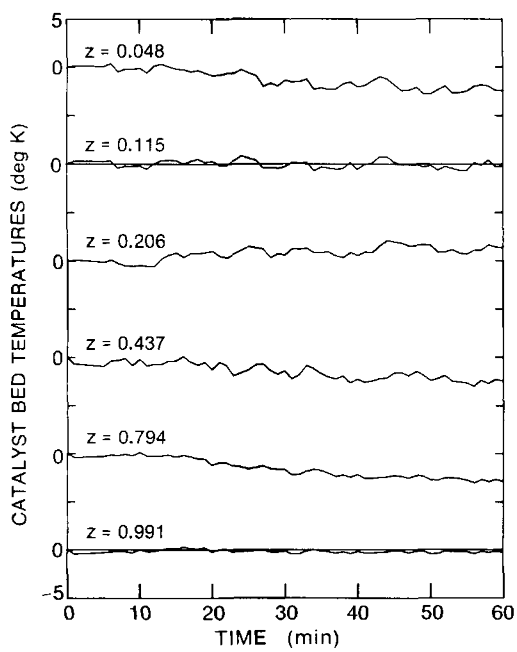

Figure 6. Response of reactor model to an 8 W step change in bottom heater.
Eq. 2 noise model used.

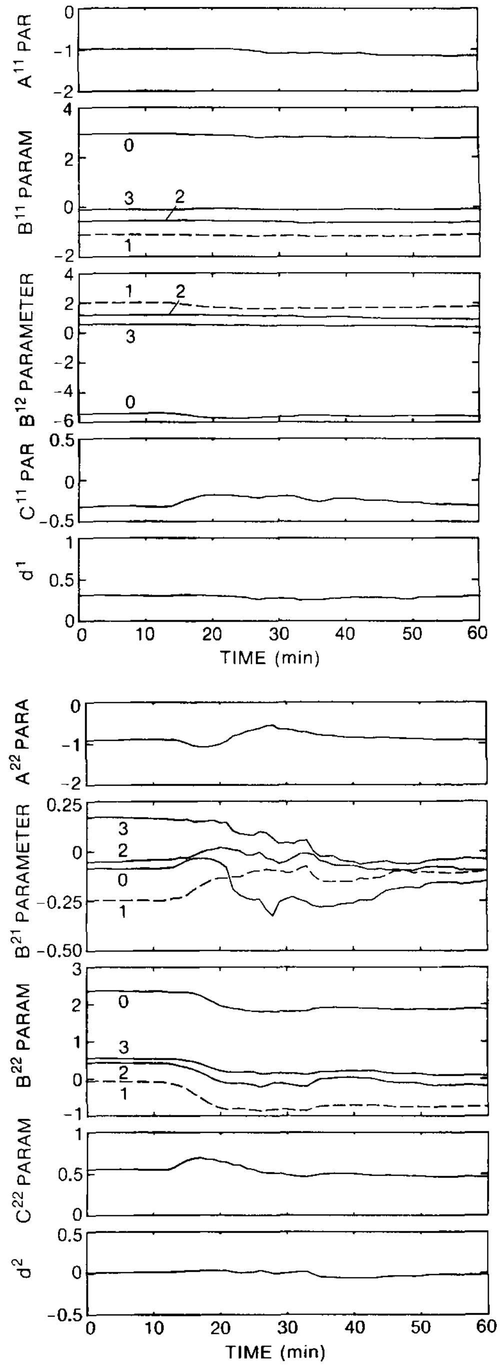

Figure 7. Behavior of model parameters for Fig. 6.

the output variances are larger than those in Figure 6. This increased output variance is a consequence of having the integrator in the loop continuously.

Figure 9 now shows that the parameter estimates for both loops are much better behaved. The B^{21} parameters are slowly changing because the top heater is not persistently exciting in this case. However, the amount of change in these parameters is not as great as in the previous case (compare Figures 7b and 9b). Both C parameters change because a new residual sequence is being used in Eq. 10, and the dynamics of this sequence are seen to be different immediately following the disturbance. In partic-

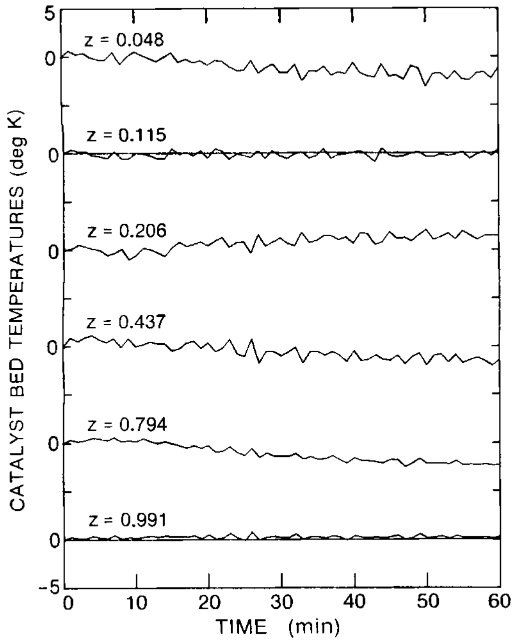

Figure 8. Response of reactor model to an 8 W step change in bottom heater.
Eq. 12 noise model used.

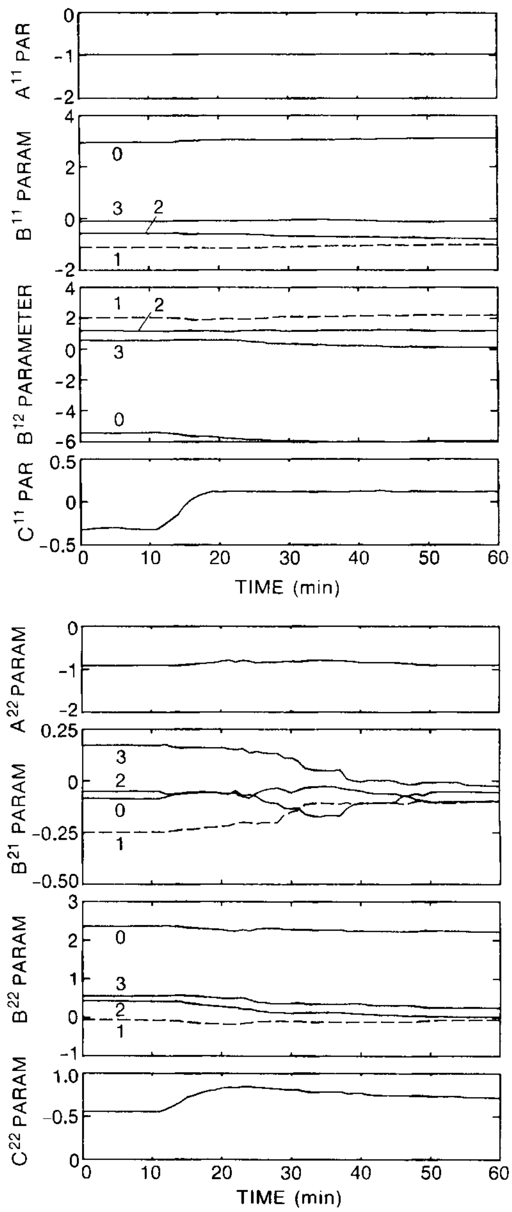

Figure 9. Behavior of model parameters for Fig. 8.

ular, the noise model (C parameters) changes immediately while the process parameters remain relatively constant.

Experimental results

We noted above that the preferred control structure for operation at the upper stable steady state is $T(z = 0.115)$ paired with the top heater, and $T(z = 0.991)$ paired with the bottom heater. In the experimental reactor the capacity of the bottom heater is approximately ± 20 W. Figure 4 showed that a bottom heater range of ± 150 W was required for control purposes. Thus, this pairing could not be tested experimentally.

However, the alternate pairing involving feed flow rate instead of bottom heater could be tested. The response of the experimental reactor for changes in each of the set points with feed flow rate as the second manipulated variable is given in Figure 10. Aside from the higher noise levels, this figure is very similar to Figure 5. Both set points are followed very closely, and the interactions are quite small. The temperature response spike that occurred when the $T(z = 0.115)$ set point returned to its original value was due to an operator error. At this time, the set point deviation was changed from -7.5 to $+7.5$ degrees (not shown), instead of 0. However, the error was corrected after one sampling instant and did not affect subsequent operations.

The amount of change required in the feed flow rate for the set point change in $T(z = 0.991)$ represented 15% of the total flow being fed into the reactor. This large change drastically affects the nonlinearities of the reactor. Nonetheless, the controller was able to deal with the change in the process dynamics very effectively. The increased activity noticeable in the input variables at the end of the run was due to the addition of the PRB signal to the calculated input signals. The fault-detection method apparently noticed a change in the process due to excitation of the nonlinearities, and a constant factor was added to the covariance matrix. This in turn caused an increase in the magnitude of the PRB signal component.

Control at the Unstable Steady State

Simulation results—Multivariable control

Figure 11 shows the response of the reactor to set point changes in each of the loops when the top heater and feed flow rate are used as the manipulated variables. As was observed at the upper stable state, both set points are tracked very well and interactions are very small. In order to eliminate the offset that was observed at the upper stable state for the set point changes, the integral controller, Eq. 10, was used in both loops for this run.

Manipulation of the feed flow rate causes the catalyst temperatures to change by altering the conversion of the primary

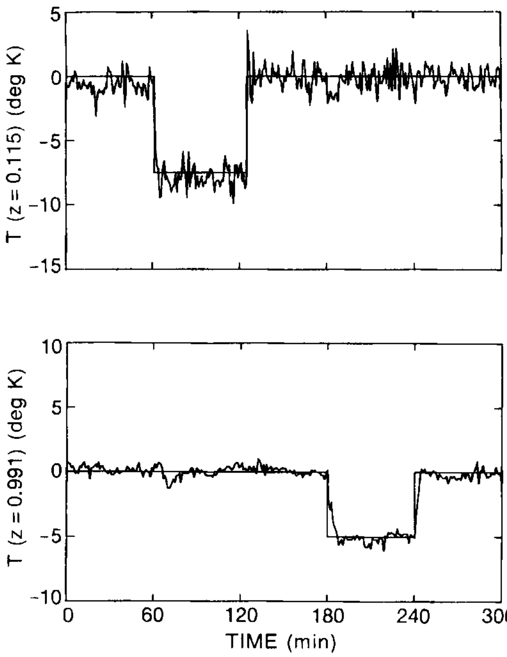

Figure 10. Response of laboratory reactor to step changes in set points.

Feed flow rate as second manipulated variable, upper stable steady state.

reactant. Hence, it follows that, at the unstable state where the steady state conversion is lower, a larger change in the flow rate should be required. A comparison of Figures 5 and 11 shows that the feed flow rate does change by a larger amount at the unstable state for the same size set point change. This behavior makes the control problem at the unstable state much more difficult, as the reactor nonlinearities become more important when these large changes in the flow rate are encountered. It is clear that the nonlinearities became particularly important at the end of the run, when the fault-detection logic noticed a change in the model and added a factor to the covariance matrix; this resulted in the magnitude of the PRB signal being increased which, in turn, shows up in the momentarily increased oscillations in both outputs at $t = 260$.

Figure 12 shows that the response of the reactor when the bottom heater is used as the manipulated variable instead of feed flow rate, is very similar to the response for the upper stable state (Figure 4). The interactions observed in $T(z = 0.115)$ are again due to the partial inability of the model to account for the large changes in the bottom heater output when the set point is changed.

A comparison of Figures 4 and 12 does not show any major difference in the amount of control action required from the bottom heater at the two steady states. This result could be expected since the dominant physical process associated with this input is heat transfer. Hence, when the bottom heater is used as the manipulated variable, no major change in the dynamics of the associated loop occurs as the reactor is moved from the upper stable state to the unstable state.

Future Experimental Program

From the simulation runs we observed that when feed flow rate is used as the second manipulated variable, approximately twice as much control action is required at the unstable state as at the upper stable state. Since the model is a reasonably good representation of the real reactor, we would expect similar

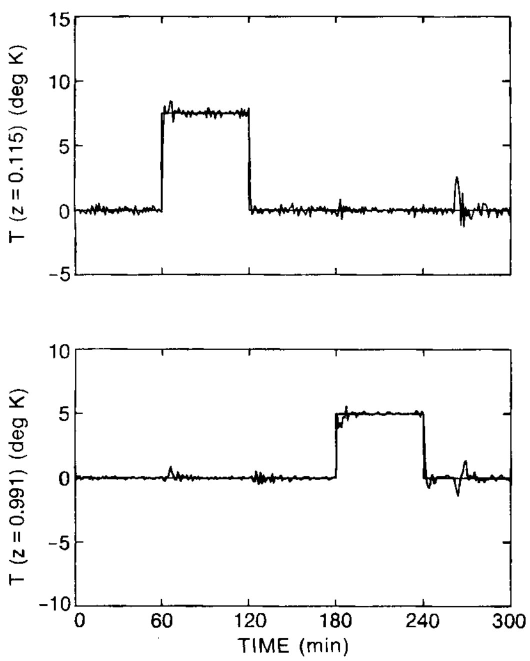

Figure 11. Response of reactor model to step changes in set points.

Feed flow rate as second manipulated variable, unstable steady state.

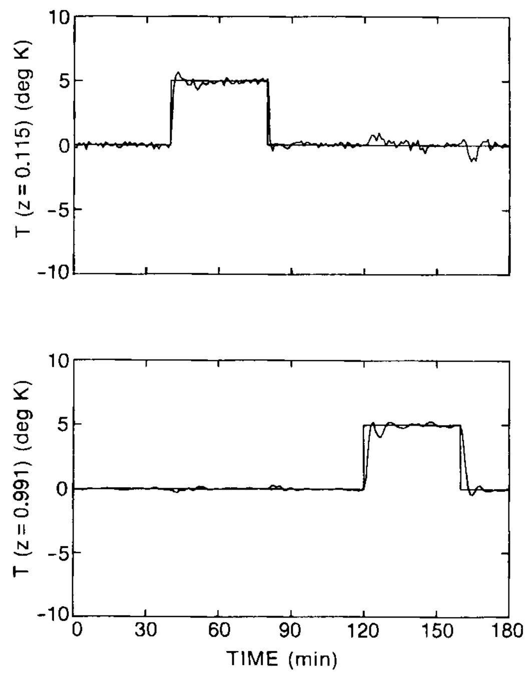

Figure 12. Response of reactor model to step changes in set points.

Bottom heater as the second manipulated variable, unstable steady state.

behavior for the experimental system. In the experimental run at the upper stable state, the large changes in feed flow rate required for control were already violating the linearity assumptions of the controller design, as well as approaching the physical constraints of the system for the flow rate. Thus, any attempt to control the reactor at the unstable state using feed flow rate would have excited the nonlinearities so much that control would not be possible (if the required flow rates could even be achieved). This pairing appears not to be feasible.

We have previously stated that the bottom heater in the experimental reactor was physically constrained so as to make controller operation at the upper stable state impossible. Figure 12 shows that at the unstable state, approximately the same amount of control action is required as at the upper stable state. For this reason, controller operation at the unstable state was also impossible. The reactor system is currently undergoing redesign so as to make the bottom heater a much more effective input. Future studies will use this input as the second manipulated variable for experimental multivariable studies at the unstable steady state.

Acknowledgment

The support of this work under National Science Foundation Grant No. CPE 81-12668 is gratefully acknowledged.

Notation

$A(z^{-1}), B(z^{-1}), C(z^{-1})$ = process model polynomials of orders n_A, n_B, and n_C, respectively.
d = offset term
$E(z^{-1}), E^{\dagger}(z^{-1}), F(z^{-1}), F^{\dagger}(z^{-1}), H(z^{-1})$ = general polynomials
I = objective function
$\underline{I}$ = identity matrix
k_{min} = minimum expected time delay
$P(z^{-1}), Q(z^{-1}), R(z^{-1})$ = objective function weighting polynomials
$S, S^{\dagger}$ = controller polynomials defined in Eqs. 5 and 10, respectively
t = time in sampling instants (integer)
T = temperature, K
T_s = sampling time
$U(t)$ = system input at time t
$V(z^{-1})$ = desired closed-loop polynomial
$X(t)$ = disturbance term, Eq. 9
$Y_r(t), Y(t)$ = system set point and output, respectively, at time t
z^{-1} = backward shift operator, $z^{-1}u(t) = u(t-1)$
z = axial distance, dimensionless
$\gamma = E(1)d$
ξ = uncorrelated random sequence of zero mean
$\phi(t + k_{min})$ = generalized output

Subscripts

D = diagonal elements
UL = upper and lower triangular elements

Literature Cited

Åström, K. J., "Self-tuning Control of a Fixed-bed Chemical Reactor System," Report IFRT-3151, Dept. of Auto. Control, Lund Inst. Tech., Lund, Sweden (1978).

Bonvin, D., and D. A. Mellichamp, "A Generalized Structural Dominance Method for the Analysis of Large-scale Systems," *Int. J. Cont.*, **35**, 807 (1982).

Bonvin, D., R. G. Rinker, and D. A. Mellichamp, "On Controlling an Autothermal Reactor at an Unstable State. I: Steady-state and Dynamic Modeling," *Chem. Eng. Sci.*, **38**, 233 (1983).

Buchholt, F., and M. Kümmel, "A Multivariable Self-tuning Regulator to Control a Double-Effect Evaporator," *Automatica*, **17**, 737 (1981).

Clement, K., S. B. Jørgensen, and J. P. Sørensen, "Fixed-bed Reactor Kalman Filtering and Optimal Control. II: Experimental Investigation of Discrete-Time Case with Stochastic Disturbances," *Chem. Eng. Sci.*, **35**, 1,231 (1980).

Dahlqvist, S. A., "Control of the Top and Bottom Product Compositions in a Pilot Distillation Column," *3rd Int. Symp. on Distillation*, Chem. Sympos. Ser., No. 56 (1979).

———, "Control of a Distillation Column Using Self-tuning Regulators," *Can. J. Chem. Eng.*, **59**, 118 (1981).

Gerry, J. P., E. F. Vogel, and T. F. Edgar, "Adaptive Control of a Pilot-Scale Distillation Column," AIChE Nat. Meet., Houston (Apr., 1983).

Hägglund, T., "Adaptive Control with Fault Detection," Report TFRT-7242, Dept. Auto. Control, Lund Inst. Tech., Lund, Sweden (1982).

Hallager, L., and S. B. Jørgensen, "Experimental Investigation of Self-tuning Control of a Gas-phase Fixed-bed Catalytic Reactor with Multiple Inputs," *Proc. 8th IFAC World Cong.*, XXII-81, Kyoto (1981).

Harris, T. J., J. F. MacGregor, and J. D. Wright, "Self-tuning and Adaptive Controllers: An Application to Catalytic Reactor Control," *Technometrics*, **22**, 153 (1980).

Jutan, A, et al., "Multivariable Computer Control of a Butane Hydrogenolysis Reactor. I: State-Space Reactor Modeling," *AIChE J.*, **23**, 732 (1977a).

Jutan, A., J. D. Wright, and J. F. MacGregor, "Multivariable Computer Control of a Butane Hydrogenolysis Reactor. II: Data Collection, Parameter Estimation, and Stochastic Disturbance Identification," *AIChE J.*, **23**, 742 (1977b).

———, "Multivariable Computer Control of a Butane Hydrogenolysis Reactor. III: On-Line Quadratic Stochastic Control," *AIChE J.*, **23**, 751 (1977c).

———, "Multivariable Stochastic Control of a Pilot-plant Packed-bed Tubular Reactor," *5th IFAC/IFIP Int. Conf. Digital Comp. Appl. to Process Control*, The Hague, Netherlands (1977d).

Koivo, H. N., J. T. Tanttu, and J. Penttinen, "Experimental Comparison of Self-tuning Controller Methods in Multivariable Case," *Proc. 8th IFAC World Cong.*, VII-53, Kyoto (1981).

Lee, K. S., and W. K. Lee, "On-line Optimizing Control of a Nonadiabatic Fixed-bed Reactor," *AIChE J.*, **31**, 667 (1985).

McDermott, P. E., "Self-tuning Control of a Fixed-bed Autothermal Reactor," Ph.D. Diss. Univ. California, Santa Barbara (1984).

McDermott, P. E., and D. A. Mellichamp, "A Decoupling Pole-placement Self-tuning Controller for a Class of Multivariable Processes," *Proc. 9th IFAC World Cong.*, Budapest (1984).

Morris, A. J., et al., "Evaluation of Self-tuning Controllers for Distillation Column Control," *Proc. 6th IFAC/IFIP Int. Conf. Digital Comp. Appl. to Process Control*, Düsseldorf, W. Germany (1980).

Morris, A. J., Y. Nazer, and R. K. Wood, "Multivariable Self-tuning Process Control," *Optimal Control Appl. Meth.*, **3**, 363 (1982).

Silva, J. M., R. H. Wallman, and A. S. Foss, "Multibed Catalytic Reactor Control Systems: Configuration Development and Experimental Testing," *Ind. Eng. Chem. Fundam.*, **18**, 383 (1979).

Sørensen, J. P., "Experimental Investigation of the Optimal Control of a Fixed-bed Reactor," *Chem. Eng. Sci.*, **31**, 763 (1977).

Sørensen, J. P., S. B. Jørgensen, and K. Clement, "Fixed-bed Reactor Kalman Filtering and Optimal Control. I: Computational Comparison of Discrete vs. Continuous Time Formulations," *Chem. Eng. Sci.*, **35**, 1,223 (1980).

Wallman, P. H., J. M. Silva, and A. S. Foss, "Multivariable Integral Controls for Fixed-bed Reactors," *Ind. Eng. Chem. Fundam.*, **18**, 392 (1979).

Wong, C., et al., "On Controlling an Autothermal Reactor at an Unstable State IV: Model Fitting and Control of the Laboratory Reactor," *Chem. Eng. Sci.*, **38**, 619 (1983).

Manuscript received July 9, 1984, and revision received Oct. 24, 1985.